Membrane lipids

Phospholipids

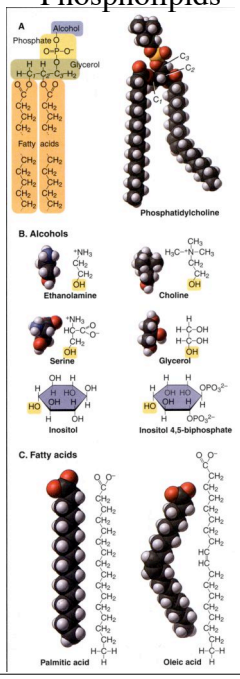

Sphingolipids

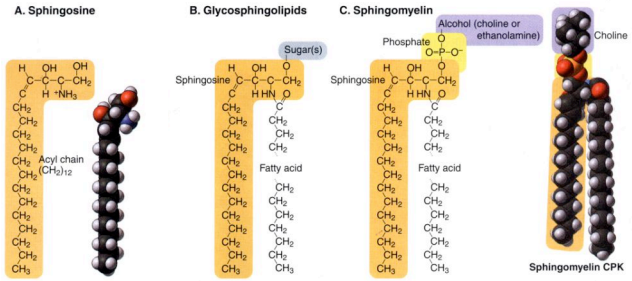

Cholesterol

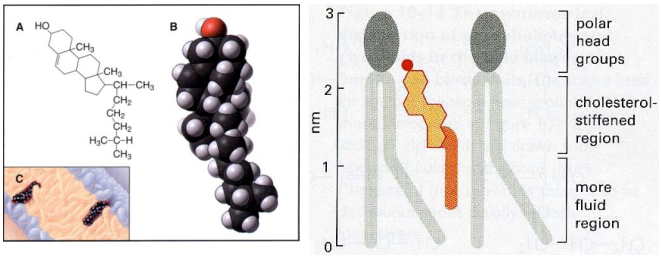

Bilayers, micelles and liposomes

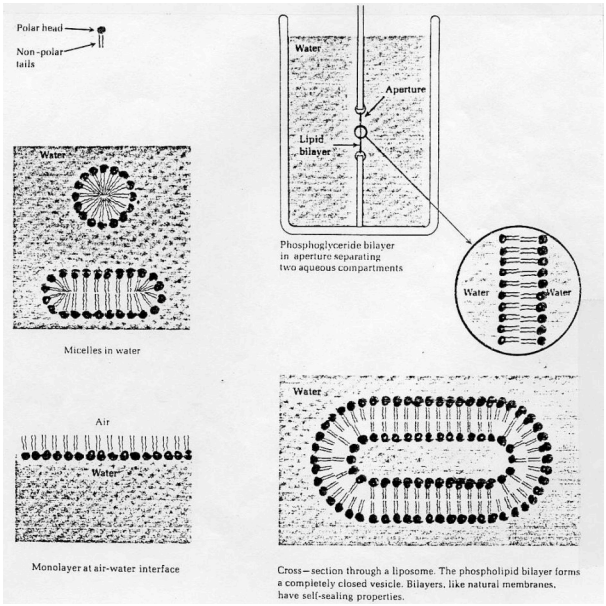

Packing of Lipids

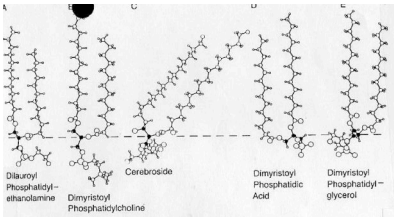

Figure 2.1. Structures of five membrane lipids as determined by X-ray crystallography. The three glycerol and sphingosine carbon backbone atoms have been colored black. Note A, B, and C have a similar conformation for the glycerol or sphingosine moiety, whereas D and E are each different. Adapted from references 604 and 636 (A); 1133 (B), 1125 (C), 594 (D) and 1126 (E). Figures kindly provided by Dr. I. Pascher.

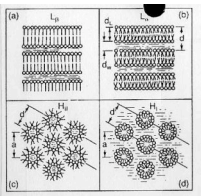

Figure 2.4. Schematic representations of lipid–water phases: (a) lamellar gel; (b) lamellar liquid crystalline; (c) hexagonal type II; (d) hexagonal type I. Various dimensions that can be measured by X-ray diffraction are indicated. Adapted from ref. 1334.

Figure 2.3. Schematic showing packing adaptations to differences in the cross-sectional areas of the polar group and the acyl chains (S and Σ_a in Figure 2.2). These figures depict the behavior of phosphatidylethanolamine and phosphatidylcholine. (A) Phosphatidylethanolamine in a crystal, where the space requirements of the headgroup and the two acyl chains are the same. (B) Phosphatidylethanolamine in a liquid crystalline lamellar phase, where the area per molecule requires that the headgroup lattice be disrupted. This will occur only if water or other polar molecules can bridge the gap between lipid neighbors and stabilize the structure. (C) Phosphatidylcholine in a hypothetical arrangement illustrating that the space required by the headgroup (50 Å^2) is substantially larger than required by the acyl chains (38 Å^2). This requires some packing adjustment. (D) One adjustment of phosphatidylcholine observed in crystals is for the headgroups to be displaced in an overlapping fashion. (E) An adjustment observed in the lamellar gel phase of phosphatidylcholine is for the chains to be tilted such that they accommodate a larger cross-sectional area (50 Å^2). (F) In the lamellar liquid crystalline phase, the size of the headgroup of phosphatidylcholine does not require the headgroup lattice to be disrupted. Adapted from ref. 604.

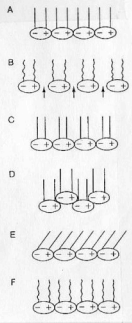

LIPID	PHASE	MOLECULAR SHAPE	CRITICAL PACKING PARAMETER (v/ℓS.)
Lysophospholipids Detergents	Micellar	Inverted Cone	<⅓ (Sphere) ⅓ to ½ (Globular Shapes; Rods)
Phosphatidylcholine Sphingomyelin Phosphatidylserine Phosphatidylinositol Phosphatidylglycerol Phosphatidic Acid Cardiolipin Digalactosyldiglyceride	Bilayer	Cylindrical	½ to 1
Phosphatidylethanolamine (Unsaturated) Cardiolipin - Ca^{2+} Phosphatidic Acid - Ca^{2+} (pH < 6.0) Phosphatidic Acid (pH < 3.0) Phosphatidylserine (pH < 4.0) Monogalactosyldiglyceride	Hexagonal (H_{II})	Cone	>1

Figure 2.18. Polymorphic phases, molecular shapes, and the critical packing parameter for some membrane lipids. Adapted from ref. 263. Drawing kindly provided by Dr. P. Cullis and Dr. M. Hope.

Detergents

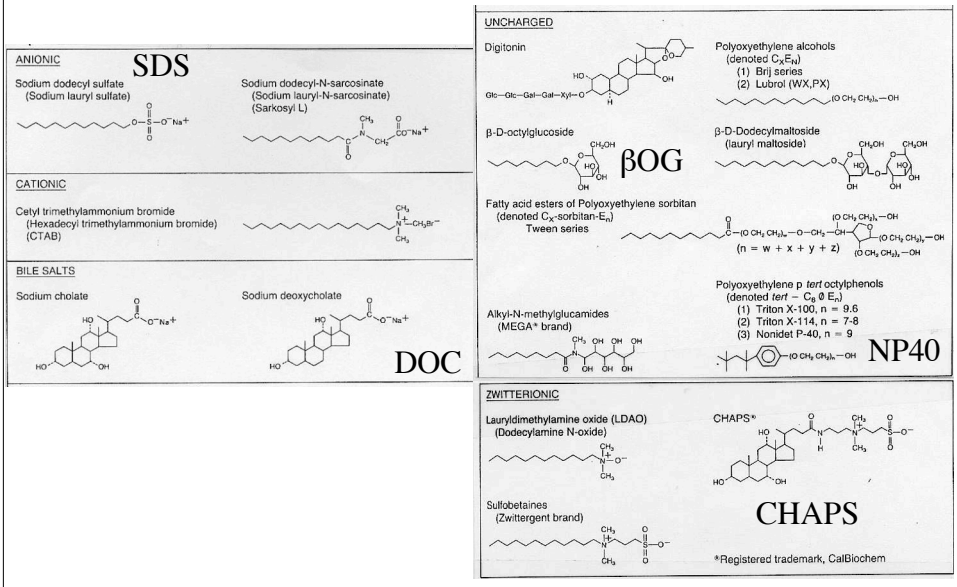

X-ray Diffraction of Lipid Bilayers & Biological Membranes

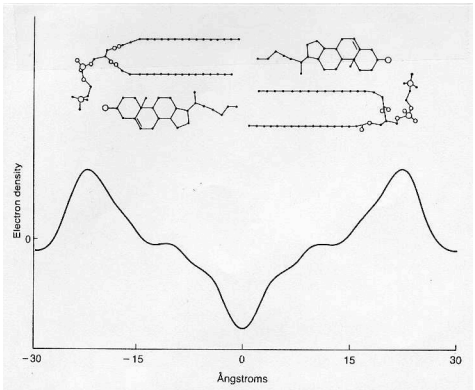

Figure 2.22. Electron density profile of a hydrated bilayer of egg phosphatidylcholine and cholesterol derived from X-ray diffraction analysis. A molecular model consistent with the data is also shown. Adapted from ref. 461.

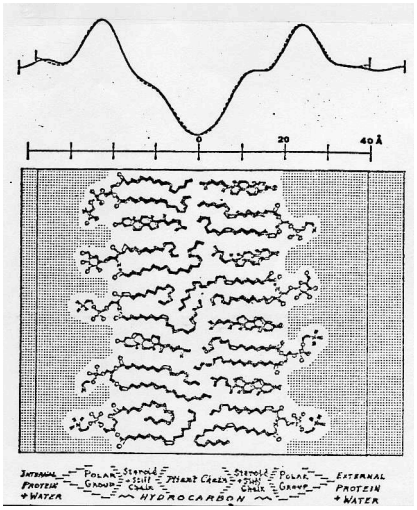

Differential Scanning Calorimetry

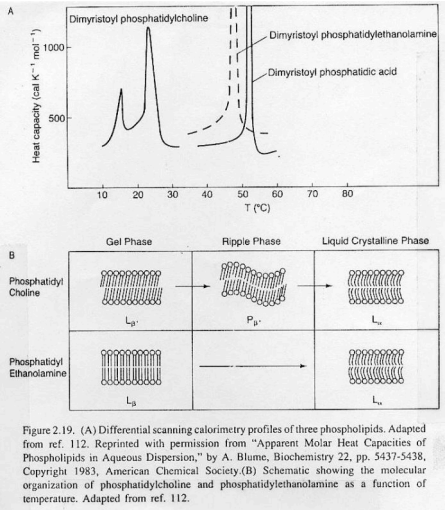

Figure 2.19. (A) Differential scanning calorimetry profiles of three phospholipids. Adapted from ref. 112. Reprinted with permission from "Apparent Molar Heat Capacities of Phospholipids in Aqueous Dispersion," by A. Blume, Biochemistry 22, pp. 5437-5438, Copyright 1983, American Chemical Society.(B) Schematic showing the molecular organization of phosphatidylcholine and phosphatidylethanolamine as a function of temperature. Adapted from ref. 112.

Electron Spin Resonance

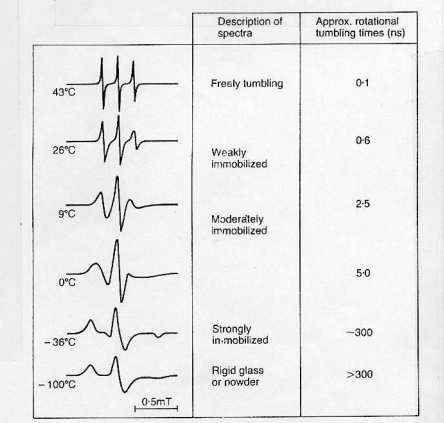

Figure 5.3. The effects of the rate of molecular rotation on the ESR spectrum of a nitroxide spin probe. These first derivative spectra were obtained by changing the temperature and, hence, the viscosity of the medium. Adapted from ref. 182.

Lipid Rafts - one example of membrane mosaicism

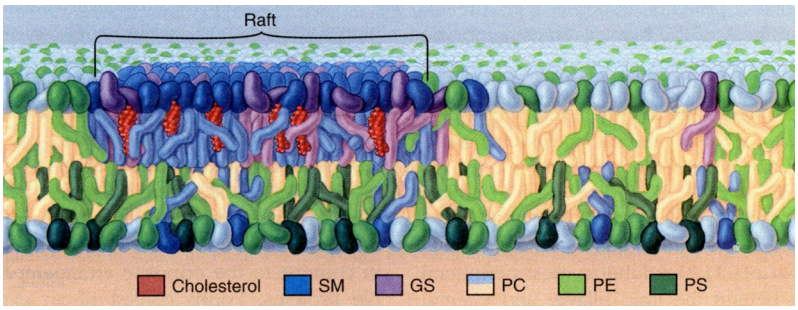

Patches of less fluid membrane enriched in sphingolipids & cholesterol

Detergent-insoluble

Less dense than bulk membrane

TEM - osmium tetroxide stain

Freeze Fracture

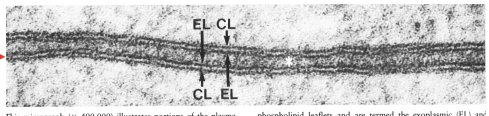

This micrograph (× 400,000) illustrates portions of the plasma membranes of two closely opposed cells. Membranes have a trilaminar structure in transmission electron micrographs. Each membrane consists of two parallel electron-dense lines separated by a lighter central zone. The electron-dense lines represent the phospholipid leaflets and are termed the exoplasmic (EL) and cytoplasmic (CL) leaflets of the plasma membrane. The exoplasmic (extracellular) leaflets contact the extracellular space (*) and the cytoplasmic leaflets contact the cytosol. The thickness of the plasma membrane is about 10 nm.

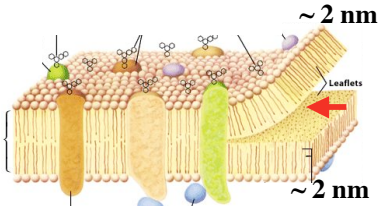

TEM - metal shadowing

IMPs - intramembranous particles - integral membrane proteins

Peripheral and Integral Membrane Proteins

Integral membrane proteins - only dissolved and handled in detergent

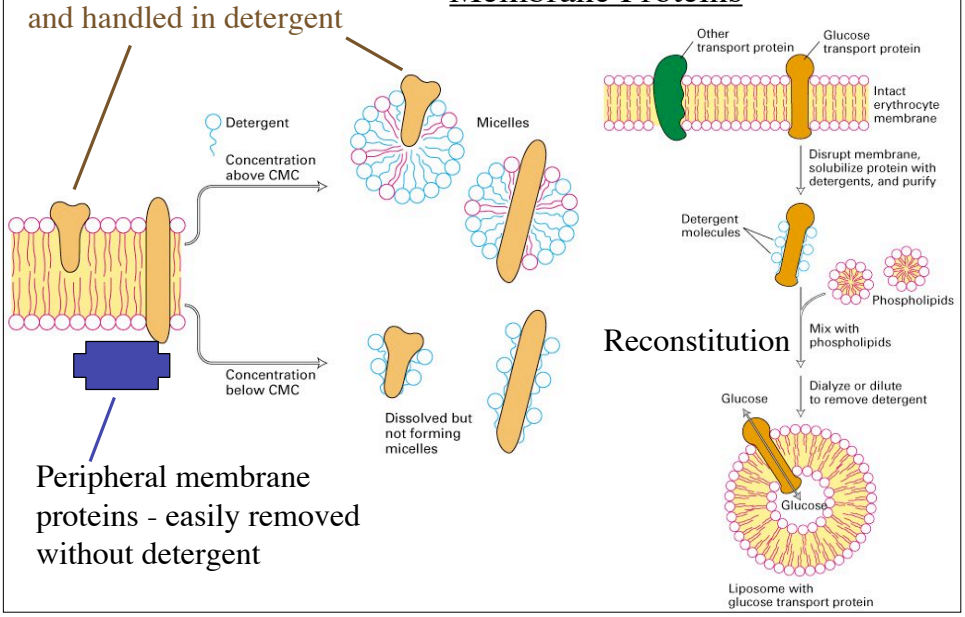

Peripheral membrane proteins - easily removed without detergent

Protein Folding in Membranes

Inside of membrane is hydrophobic
Residues contacting lipid side chains need to be hydrophobic
There is an energy cost associated with introducing charged or hydrophilic residues into the hydrophobic bilayer.

On balance ΔG must be < 0
Free energy balance sheet - some examples

20 x F residues	~ 30 kcal/mole GAIN
Ionized group	~ 25-40 kcal/mole
Ion pair	~ 10-15 kcal/mole
Hydroxyl group	~ 4 kcal/mole
One unsatisfied H bond	~ 5 kcal/mole
Therefore - a 3-4 residue turn	~ 15-20 kcal/mole

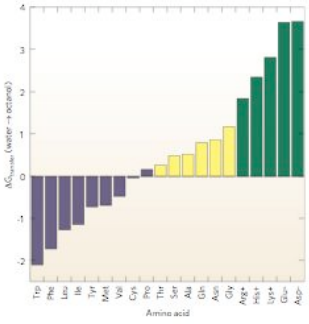

Protein Folding in Membranes

α-helix	3.6 residues per turn, 1.5 A/residue 20-22 residues to cross membrane H-bonds satisfied within one helix Often a hydrophobic stretch
β-sheet	2 residues per turn, 3.3 A/residue 7-9 residues to cross membrane H-bonds only satisfied in multiple strands Rarely detectable as a hydrophobic stretch

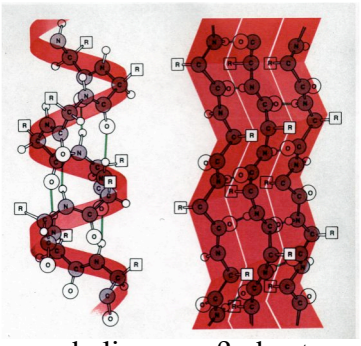

α-helix β-sheet

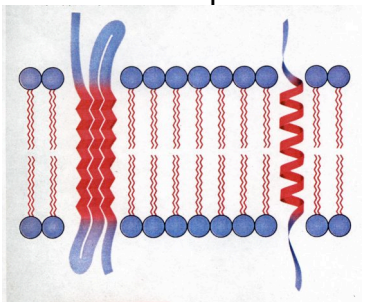

Transmembrane segments

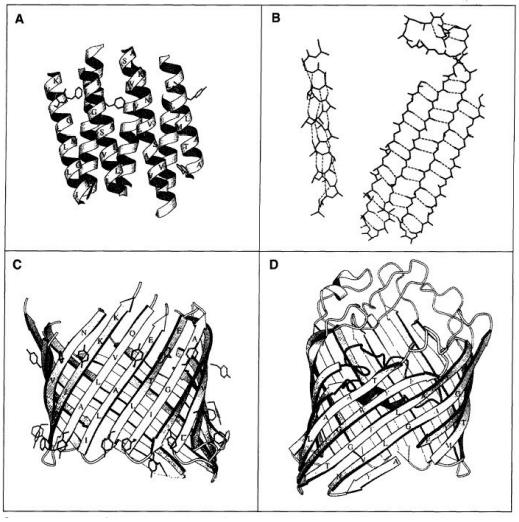

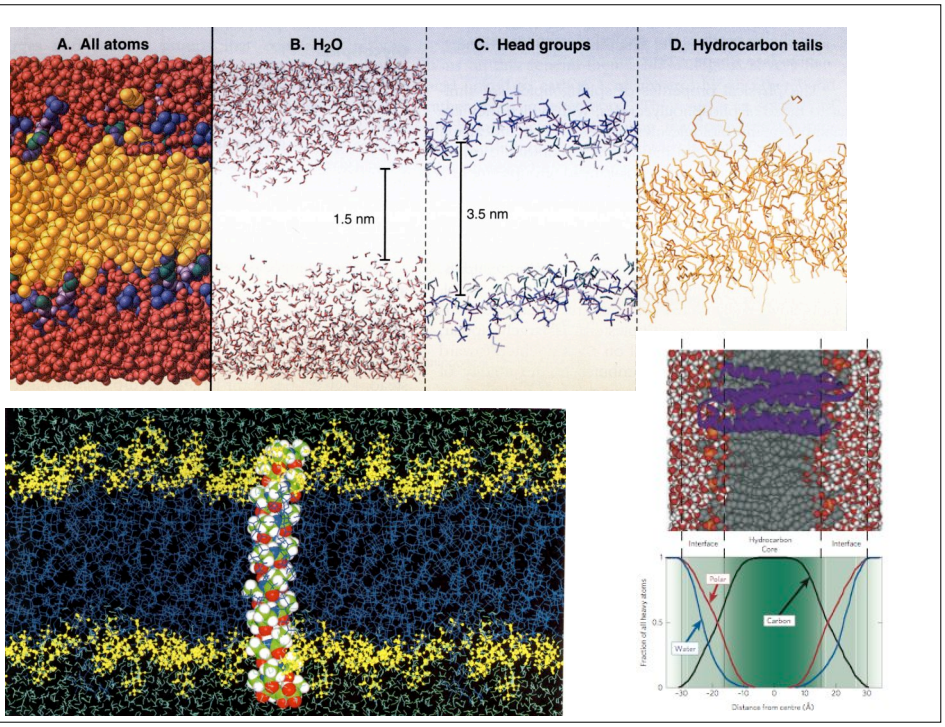

Membrane Proteins

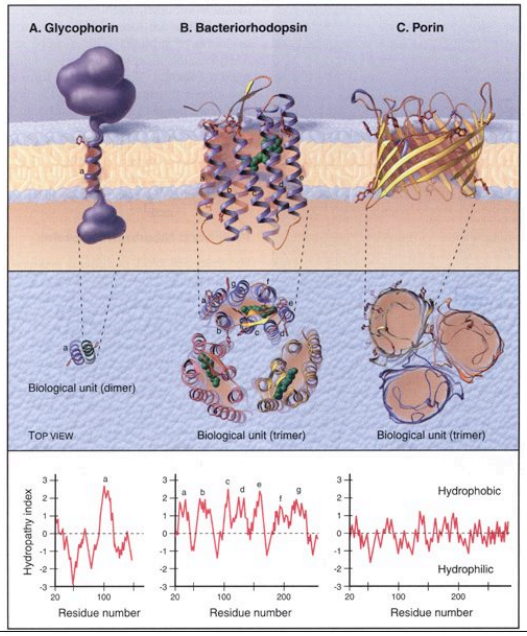

Side views

Plan views

Hydropathy plots

BACTERIAL RHODOPSIN

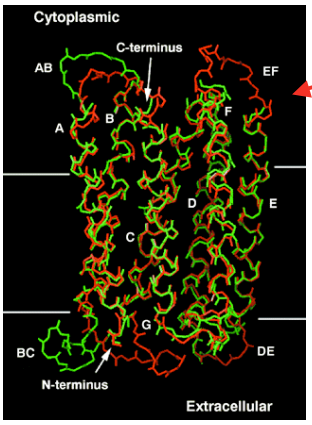

Side views

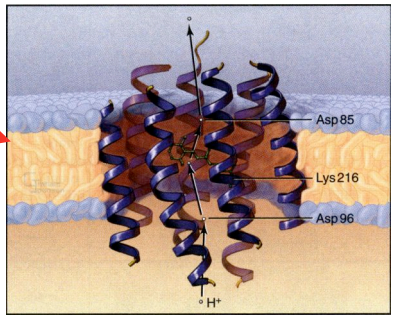

X-ray structure

EM structure

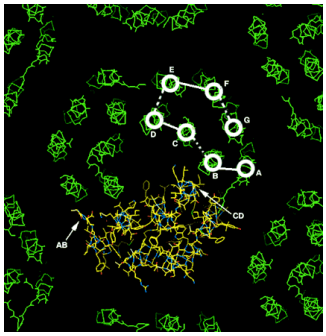

Plan view

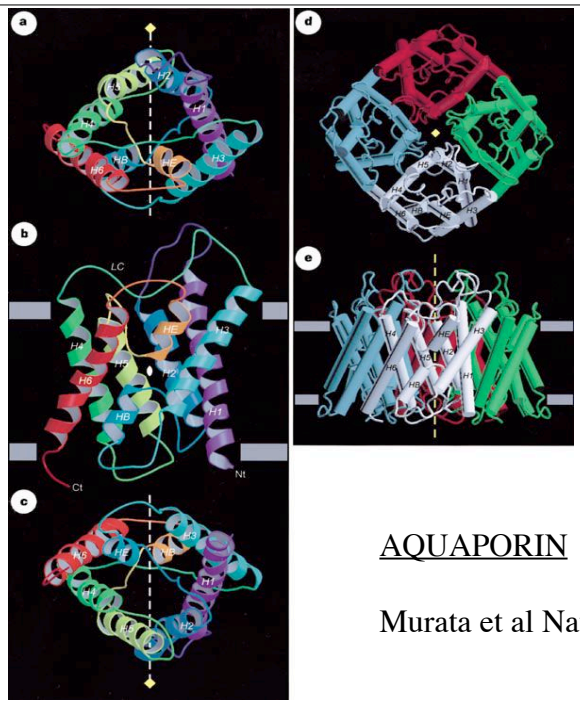

monomer - side view

tetramer - top view

tetramer - side view

AQUAPORIN

Murata et al Nature 2000

Cyanobacterial Photosystem I

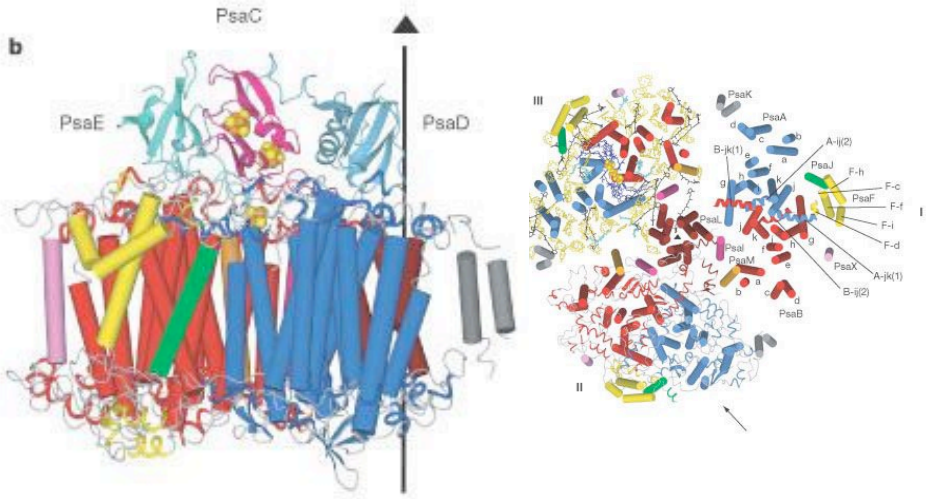

Bacterial porins

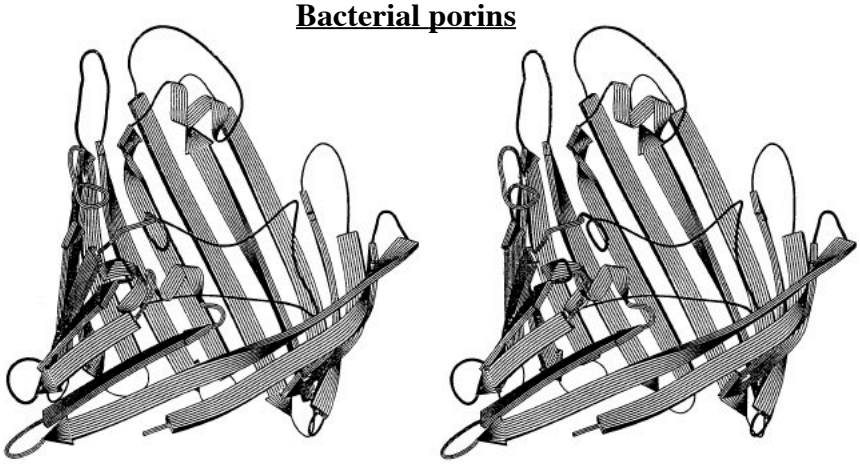

Fig. 1. Stereo view of the chain fold of one subunit of the porin of *Rhodobacter capsulatus* as drawn with the program RIBBON (*31*). Indicated are β strands (arrows) and α helices. The view is approximately from the threefold axis. The amino and carboxyl termini are adjacent and at the front side. The large loop between strands β5 and β6 lining the inside of the 16-stranded β barrel forms the solute size defining eyelet of the pore. Clearly visible is the smooth-rimmed bottom end of the barrel, which faces the periplasm, and the rugged top end, which faces the external medium (*29*, *30*).

Nicotinic Acetylcholine Receptor

Structure determined by electron Crystallography to 4A resolution

Miyazawa, Fujiyoshi & Unwin Nature 423: 949-955 (2003)

Unwin, J.Mol.Biol. 346:967-989 (2005)

Each subunit contributes an α-helix to the pore and three to the surround

Extracellular domain is homologous with an acetylcholine-binding protein from a snail

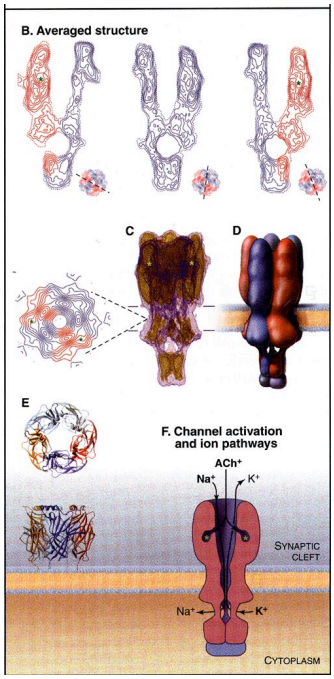

Nicotinic Acetylcholine Receptor

Structure determined by electron Crystallography to 4A resolution

Miyazawa, Fujiyoshi & Unwin Nature 423: 949-955 (2003)

Unwin, J.Mol.Biol. 346:967-989 (2005)

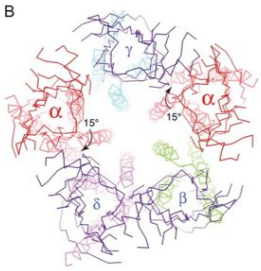

Binding of ACh causes 15° rotation and opens gate in middle of membrane

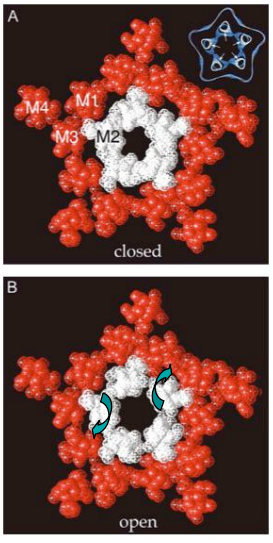

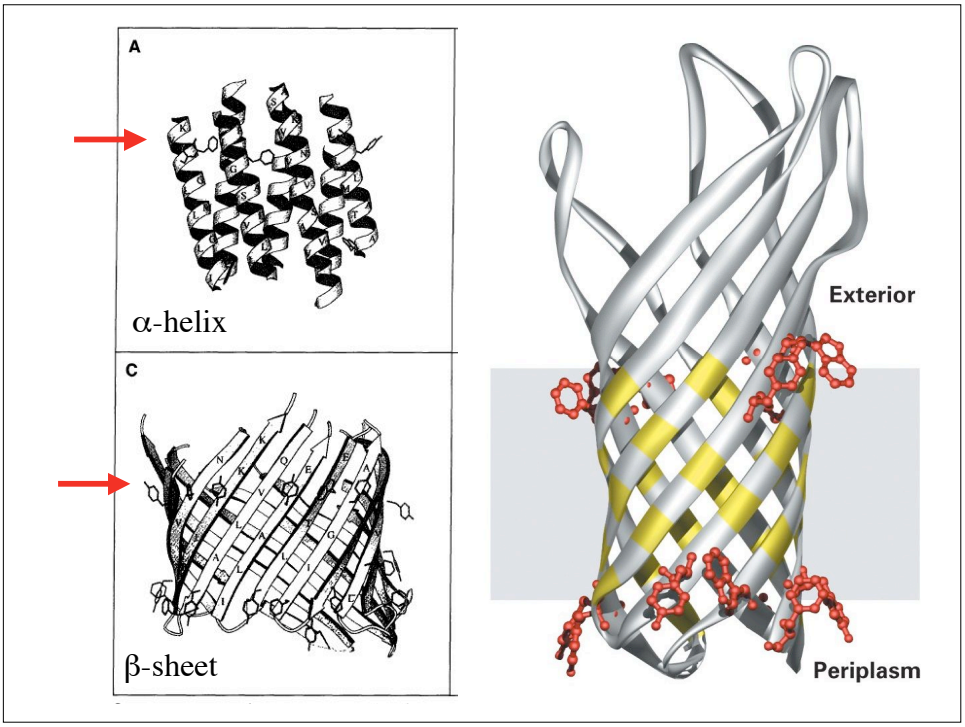

Predicting Transmembrane Topography

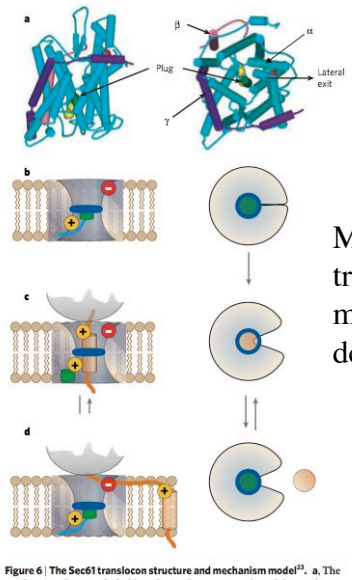

Figure 6 | The Sec61 translocon structure and mechanism model[23]. a, The

Maybe the translocon makes this determination?

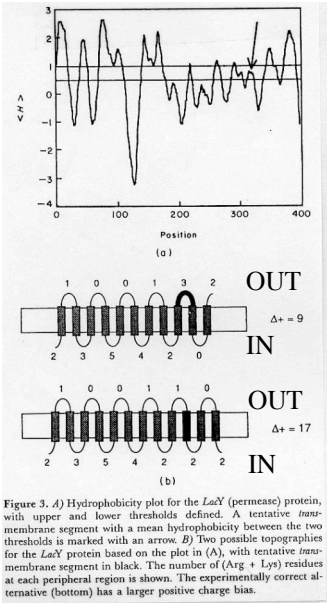

Figure 3. *A)* Hydrophobicity plot for the *LacY* (permease) protein, with upper and lower thresholds defined. A tentative *trans*-membrane segment with a mean hydrophobicity between the two thresholds is marked with an arrow. *B)* Two possible topographies for the *LacY* protein based on the plot in (A), with tentative *trans*-membrane segment in black. The number of (Arg + Lys) residues at each peripheral region is shown. The experimentally correct alternative (bottom) has a larger positive charge bias.

"Positive-inside" rule
Nilsson and von Heijne
Cell 62:1135-1141 (1990)

Testing TransmembraneTopography

Proteolysis

Antibodies

Surface Labeling

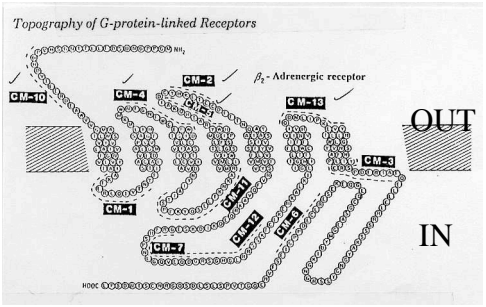

Surface Labeling Reagents

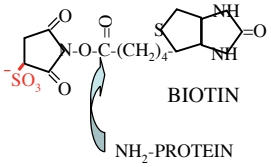

(sulfo)NHS-BIOTIN

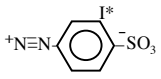

Diazotized Iodo-sulfanilic acid

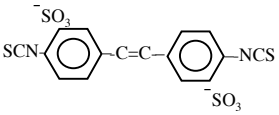

Diisothiocyanostilbene-2,2' disulfonate (DIDS)

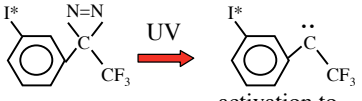

Trifluoro methyl-3 iodoaryldiazirine (^{125}I-TID)
hydrophobic, membrane soluble

Testing TransmembraneTopography

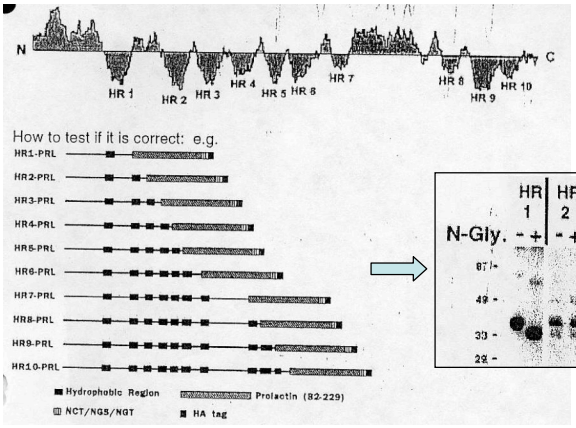

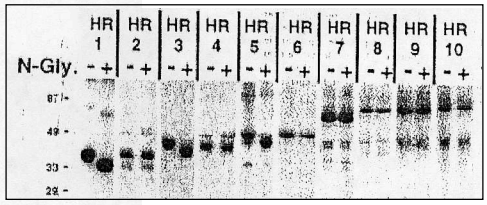

Lehmann et al
JBC 272:12047-51 (1997)
Evidence for a six transmembrane domain structure of presenilin 1

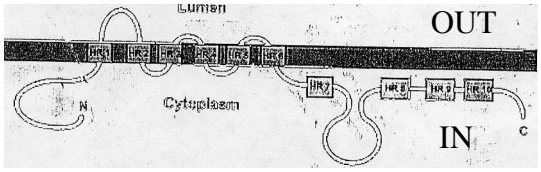

Lipid Modifications of Membrane Proteins #1

A. **Phosphatidyl inositol glycan** (PIG-tailed, PI-linked)

- Attached near C-terminus - signalled by a short hydrophobic stretch which is removed.
- Linkage is via ethanolamine to carboxyl terminus-amide bond; irreversible
- Anchors external membrane proteins in external leaflet via two acyl chains.
- Connection can be cleaved by PI-specific phospholipase C.
- This is only known external connection - others provide insertion into internal leaflet.

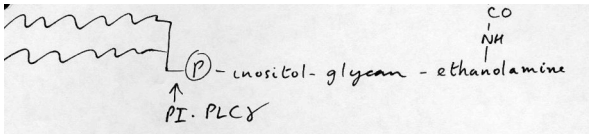

B. **Myristoylation**

- 14C fatty acid (myristate) attached via amide bond to N-terminal glycine.
- There is a recognition sequence internal to N-terminal glycine.
- Amide linkage is irreversible.
- Confers some affinity for membranes
  (~8kcal/mole, equivalent to inserting 10 CH_2 in the hydrophobic base Kd ≅ 10^{-4} M).
- This is insufficient for efficient membrane localization.
- Myristoylation is usually coupled with other elements conferring membrane-binding
  eg, basic amino acids or palmitoylation.

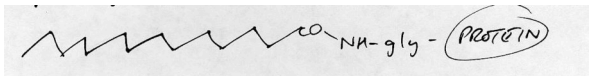

Lipid Modifications of Membrane Proteins #2

C. Palmitoylation

- Attachment of 16C fatty acid (palmitate) to cysteine residue via S-acyl linkage - reversible.
- Often associated with irreversible modification (myristoylation or prenylation) at nearby residues.
- Palmitoylation adds membrane-binding affinity.

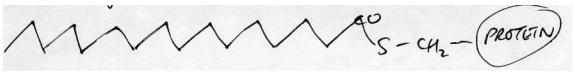

D. Prenylation

- Attachment of a prenyl group(isoprenoid) to a cysteine residue very near the C-terminus.
- The C is located in the sequence CAAX (or variants thereof)
  where X is any amino acid and A is a hydrophobic residue.
  The AXX sequence is removed by proteolysis and the carboxyl of the cysteine is methylated.
- The linkage is via a thioether (-CH-S-) bond and is irreversible.
- Two prenyl groups are found: farnesyl (15C) or, more commonly, geranyl geranyl (20C)
  attached by different prenyl transferases recognizing different CAAX sequences.
- Prenylation is frequently associated with palmitoylation at nearby cysteines.

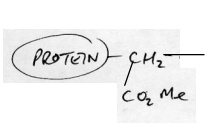

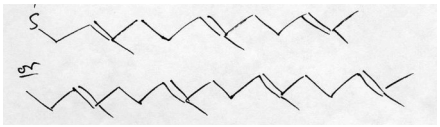

farnesyl (15C)

geranyl geranyl (20C)

Multiple ways for membrane proteins to associate with the membrane

Lipid-linked

Peripheral - binding to phospholipid head groups

Integral
- partially inserted
- single pass TM
- multiple pass TM

Peripheral - binding to integral proteins

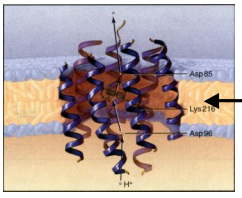

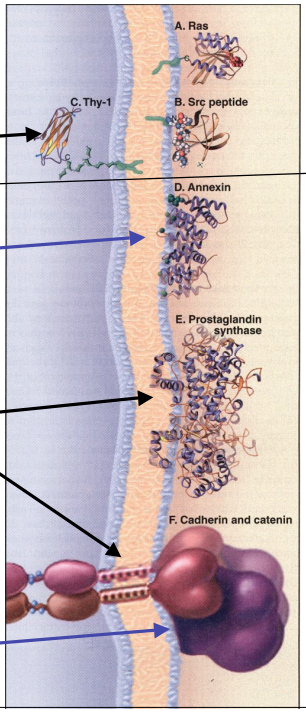

The not-so-fluid mosaic membrane

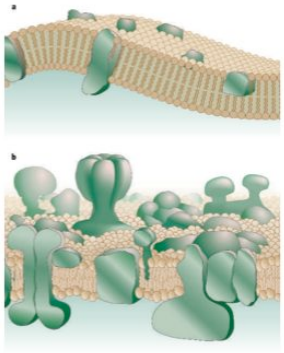

Figure 1 | General models for membrane structure. a, The Singer–Nicholson 'fluid mosaic model' (ref. 1). b, An amended and updated version.

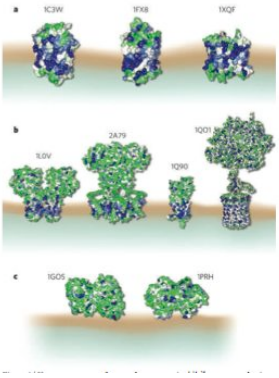

Many membrane proteins occlude lipid

Many protein oligomers

Bilayer thickness varies

Engelman DM (2005) Membranes are more mosaic than fluid. Nature 438:578-580.

Lateral Mobility of Membrane Proteins

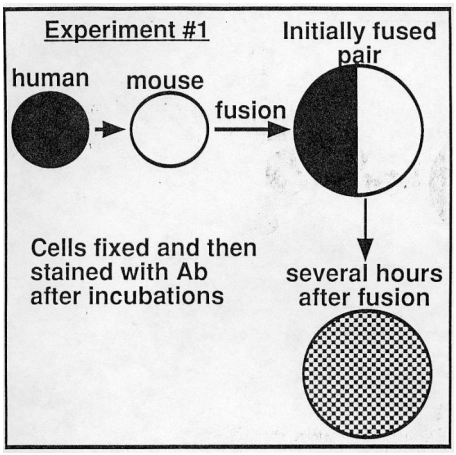

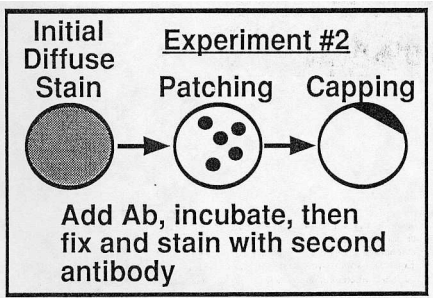

Fluorescence Recovery after Photobleaching (FRAP)

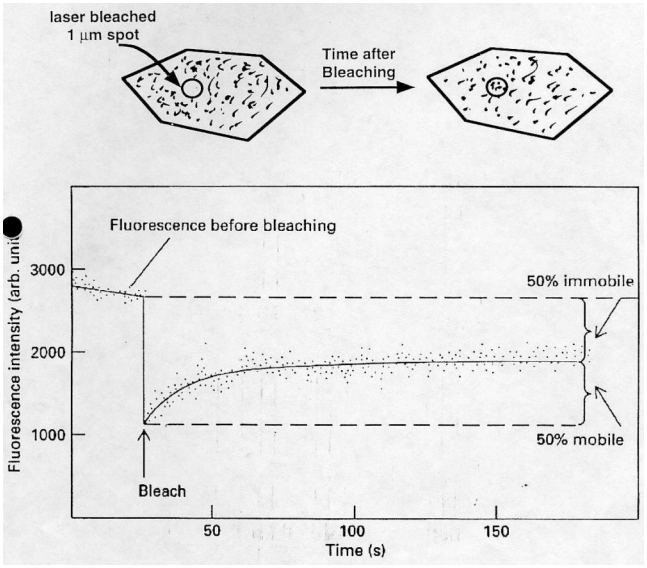

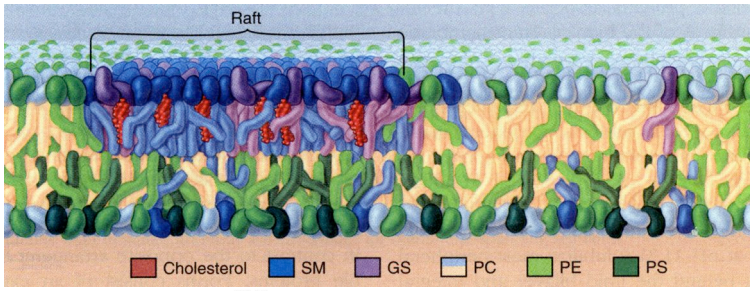

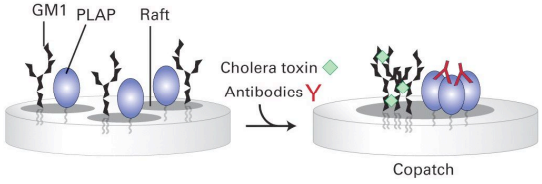

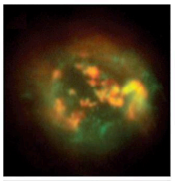

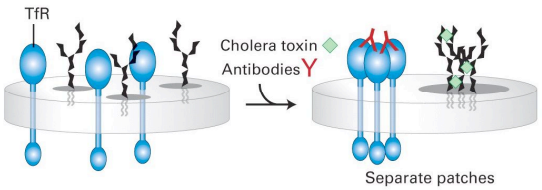

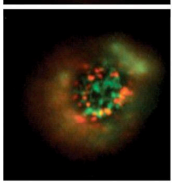

Restrictions on Lateral Mobility of Membrane Proteins

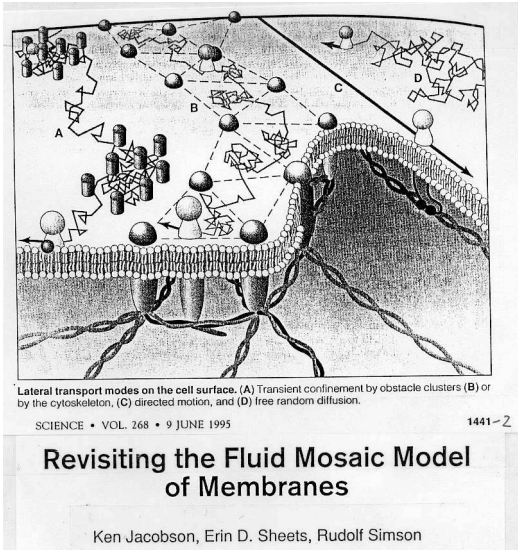

Single particle tracking and optical tweezers reveal restrictions on lateral mobility of integral membrane proteins.

Submembrane cytoskeleton of red blood cells

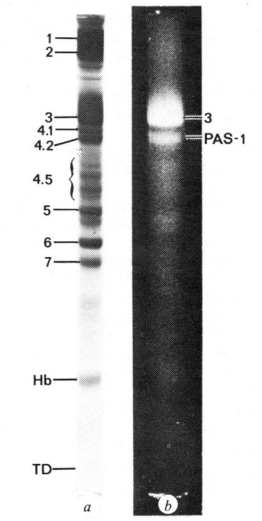

Protein CHO

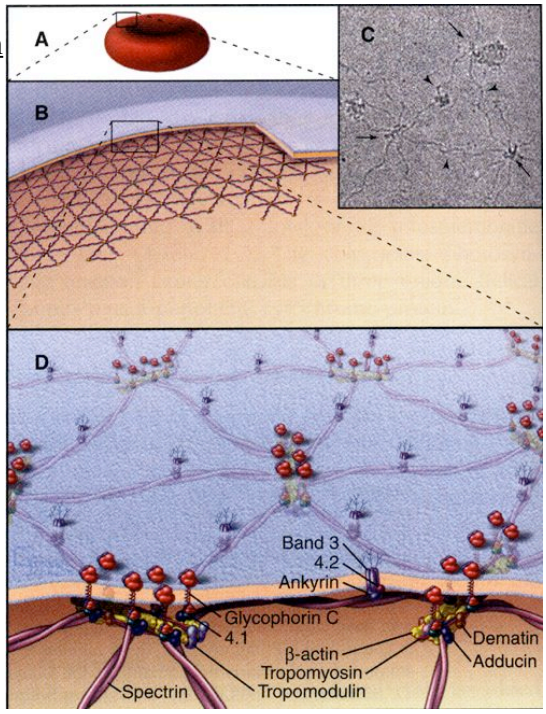

Dissection of the Erythrocyte Membrane

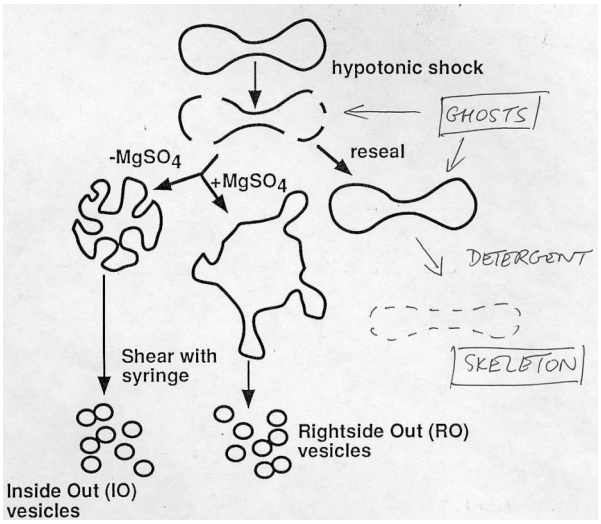

Dissection of the Erythrocyte Membrane

GHOSTS

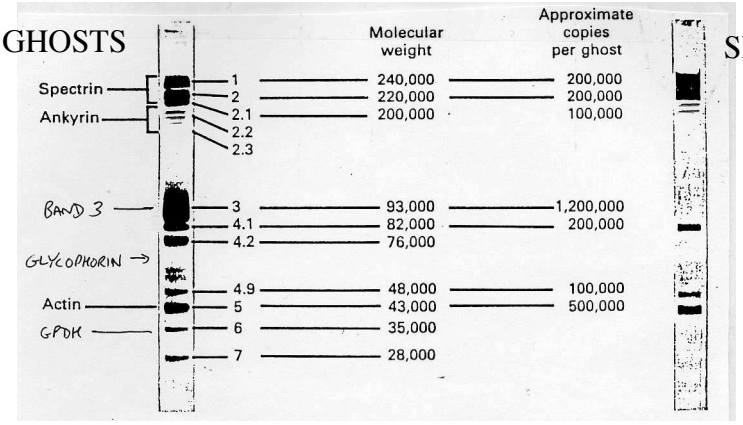

SKELETONS

Detergent extracts - Band 3, glycophorin - INTEGRAL
Low salt extracts - Spectrin (1,2) and actin (5)
High salt extracts - ankyrin (2.1, 2.2) and band 4.1
} - PERIPHERAL

Spectrin

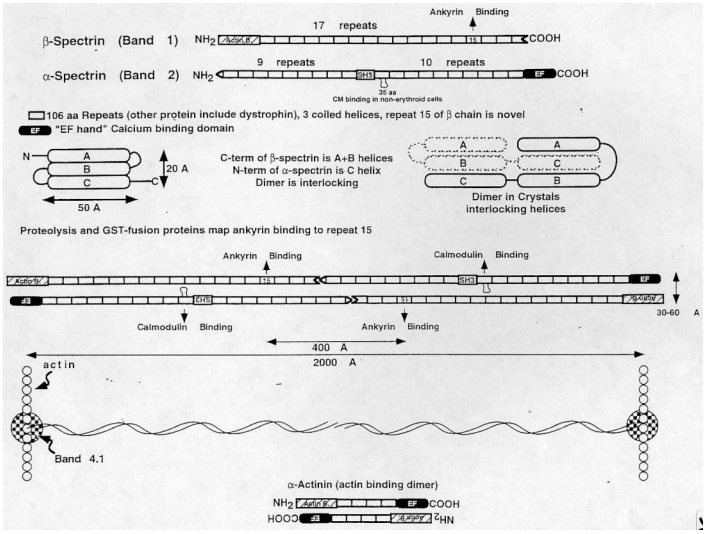

Human mutations in spectrin, ankyrin and band 3 produce defective red cells

2-ply Organization of Erythrocyte Membranes

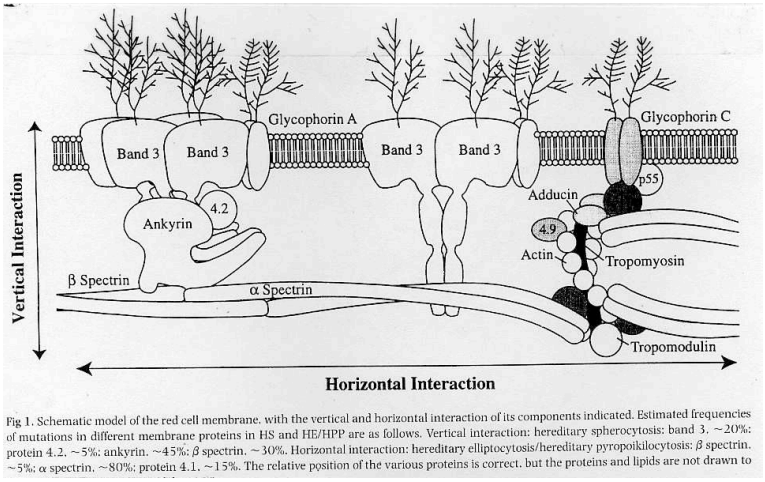

Fig 1. Schematic model of the red cell membrane, with the vertical and horizontal interaction of its components indicated. Estimated frequencies of mutations in different membrane proteins in HS and HE/HPP are as follows. Vertical interaction: hereditary spherocytosis: band 3, ~20%; protein 4.2, ~5%; ankyrin, ~45%; β spectrin, ~30%. Horizontal interaction: hereditary elliptocytosis/hereditary pyropoikilocytosis: β spectrin, ~5%; α spectrin, ~80%; protein 4.1, ~15%. The relative position of the various proteins is correct, but the proteins and lipids are not drawn to

Lux and Palek 1995 How relevant is this to other membranes?

Restrictions on Lateral Mobility of Membrane Proteins in Other Cells

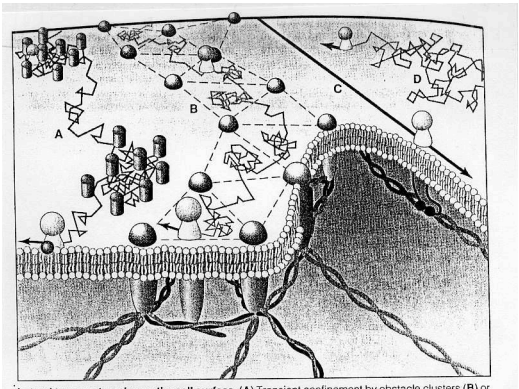

Lateral transport modes on the cell surface. (**A**) Transient confinement by obstacle clusters (**B**) or by the cytoskeleton, (**C**) directed motion, and (**D**) free random diffusion.

SCIENCE • VOL. 268 • 9 JUNE 1995 1441

Revisiting the Fluid Mosaic Model of Membranes

Ken Jacobson, Erin D. Sheets, Rudolf Simson

EM analysis of submembranous cytoskeleton

Morone…Kusumi et al J. Cell Biol. 2006

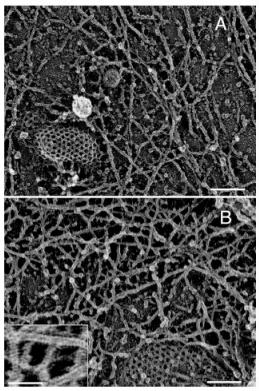

Figure 2. **Magnified MSK images of an NRK and FRSK cell on the cytoplasmic surface of the upper membrane.** (A) NRK cell; (B) FRSK cell. Clathrin-coated structures (A and B) and a caveola (A) show the cytoplasmic surface. The striped banding patterns with the 5.5-nm periodicity on individual filaments are characteristic of actin filaments. These images also reveal close links of the MSK actin filaments with the clathrin-coated structures and caveolae. Bars (A and B), 100 nm; (inset) 50 nm.

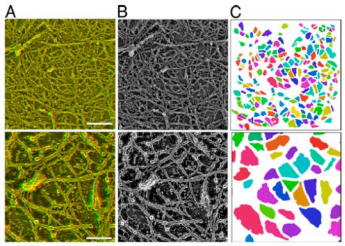

Figure 7. **The MSK meshwork directly on the cytoplasmic surface of the plasma membrane.** The central parts of the figures in the top row (bar, 300 nm) are magnified by a factor of three and are shown in the bottom row (bar, 100 nm). (A) Typical stereo views of the plasma membrane specimen (anaglyph; left = red). (B) Normal electron micrographs of the plasma membrane samples. The same view fields as those in A. (C) The areas delimited by the actin filaments closely opposed to the cytoplasmic surface of the cell membrane are shown. Different colors are shown to help the eye.

EM tomography of freeze, deep-etched and shadowed samples gives 3D image of membrane skeleton. Can see domains (above) and correlate their size distribution with sizes determined by single particle tracking

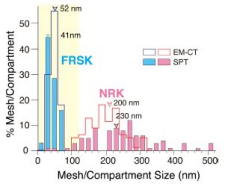

Figure 8. **Comparison of the distributions of the MSK mesh size on the cytoplasmic surface of the plasma membrane estimated by electron tomography with that of the compartment size determined from the phospholipid diffusion data for NRK and FRSK cells.** Electron tomography, open bars; phospholipid diffusion data, closed bars (adapted from Fujiwara et al., 2002 and Murase et al., 2004). NRK, pink; FRSK, blue. Within the same cell type, the MSK mesh size and diffusion compartment size exhibited similar distributions (compare the open and closed bars with the same color). The actual sizes are quite different between NRK and FRSK cells. EM-CT, EM-based computer tomography; SPT, single-particle tracking.

RHODOPSIN

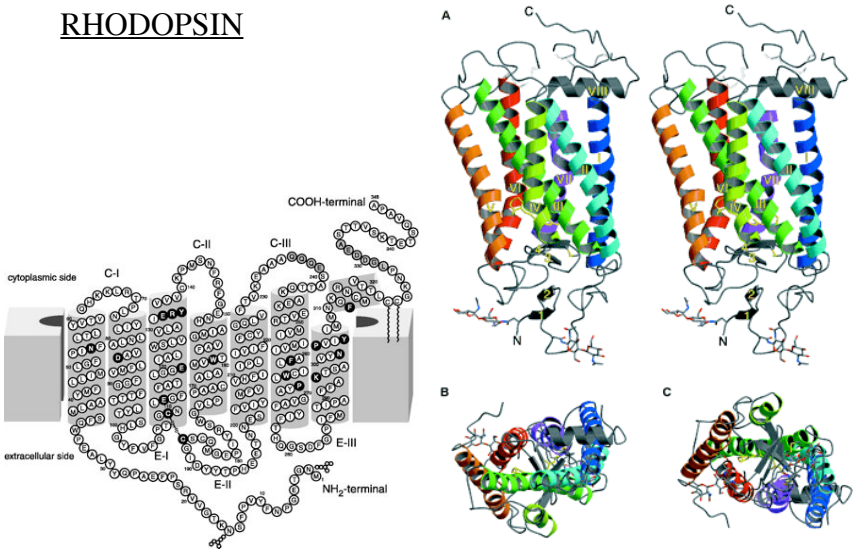

Mutations in Spectrin & other Erythrocyte Membrane Proteins

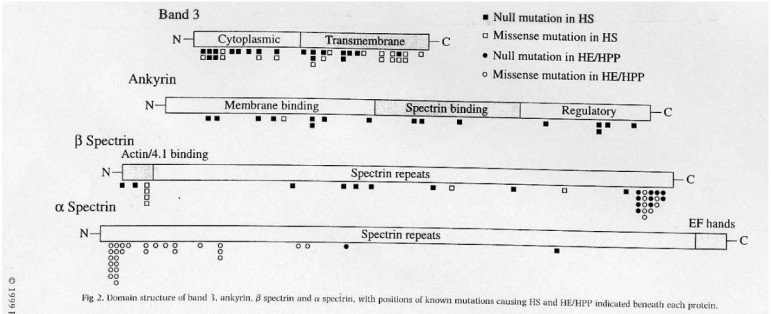

Fig 2. Domain structure of band 3, ankyrin, β spectrin and α spectrin, with positions of known mutations causing HS and HE/HPP indicated beneath each protein.

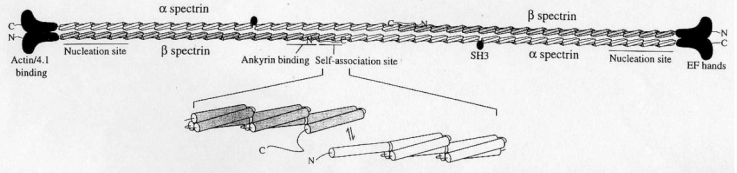

Fig 3. Structure of the spectrin tetramer, showing the triple helical coiled-coil repeats of the spectrin peptides, the head-to-head spectrin self-association sites, and the nucleation sites that initiate the side-to-side interaction between α and β spectrin chains.